Efficient Sorting of Orbital Angular Momentum States of Light

Gregorius C. G. Berkhout,[1,2,*] Martin P. J. Lavery,[3,†] Johannes Courtial,[3] Marco W. Beijersbergen,[1,2] and Miles J. Padgett[3]

[1]*Huygens Laboratory, Leiden University, P.O. Box 9504, 2300 RA Leiden, The Netherlands*
[2]*cosine Science & Computing BV, Niels Bohrweg 11, 2333 CA Leiden, The Netherlands*
[3]*School of Physics and Astronomy, University of Glasgow, Glasgow, United Kingdom*
(Received 19 July 2010; published 4 October 2010)

We present a method to efficiently sort orbital angular momentum (OAM) states of light using two static optical elements. The optical elements perform a Cartesian to log-polar coordinate transformation, converting the helically phased light beam corresponding to OAM states into a beam with a transverse phase gradient. A subsequent lens then focuses each input OAM state to a different lateral position. We demonstrate the concept experimentally by using two spatial light modulators to create the desired optical elements, applying it to the separation of eleven OAM states.

Nearly twenty years ago it was recognized by Allen *et al.* that helically phased light beams, described by a phase cross section of $\exp(i\ell\phi)$, carry an orbital angular momentum (OAM) of $\ell\hbar$ per photon, where ℓ can take any integer value [1–3]. The unlimited range of ℓ gives an unbounded state space, and hence a large potential information capacity [4,5]. At the level of single photons, OAM entanglement is a natural consequence of the conservation of angular momentum in nonlinear optics [6]. This entanglement makes OAM a potential variable for increased-bandwidth quantum cryptography [7–9], but only if a single photon can be measured to be in one of many different states.

Generation of helically phased beams with OAM is most usually accomplished using a diffractive optical element, i.e., hologram, the design of which is a diffraction grating containing an ℓ-fold fork dislocation on the beam axis [10,11]. If the hologram is illuminated by the output from a laser, or single-mode fiber, the first-order diffracted beam has the required helical phase structure. The same setup, when used in reverse, couples light in one particular OAM state into the fiber. In this case, the hologram acts as a mode specific detector, working even for single photons [12]. However, such a hologram can only test for one state at a time. Testing for a large number of possible states requires a sequence of holograms, thereby negating the potential advantage of the large OAM state space. More sophisticated holograms can test for multiple states, but only with an efficiency approximately equal to the reciprocal of the number of states [5,13]. For classical light beams, the OAM state can be readily inferred by the interference of the beam with a plane wave and counting the number of spiral fringes in the resulting pattern [14]. One can also use the diffraction pattern behind specific apertures to determine the OAM state of the incoming light beams [15,16]. All of these approaches again require many photons to be in the same mode so as to produce a well-defined pattern.

The symmetry of helically phased beams means that their rotation about the beam axis induces a frequency shift, each OAM component inducing a separate frequency sideband [17], which could, in principle, be used to measure OAM [4]. However, spinning a beam about its own axis at a rate sufficient to measure its frequency shift is not technically possible. This technical challenge is lessened by using a static beam rotation to introduce an ℓ-dependent phase shift within a Mach-Zehnder interferometer; a cascade of $N - 1$ interferometers can measure N different states [18]. Although establishing the principle for single-photon measurement of OAM, for large N, this cascaded interferometric approach remains technically demanding for inclusion into larger systems.

In this Letter we are motivated by the simple example of the discrimination of plane waves within direction space. A lens is all that is required to focus a plane wave to a spot in its focal plane, the transverse position depending on the transverse phase gradient of the plane wave. This allows multiple plane waves to be distinguished from each other using a detector array. A requirement for the separation of any two plane waves is an additional phase change of 2π across the aperture of the lens, resulting in a difference in spot positions comparable to the Rayleigh resolution limit. This suggests an approach for separating OAM states, for which a change in mode index of $\Delta\ell = 1$ corresponds to an increment in the azimuthal phase change of 2π. The key optical component in this approach is one that transforms azimuthal position in the input beam into a transverse position in the output beam, i.e., an optical element that transforms a helically phased beam into a transverse phase gradient. This corresponds to the transformation of an input image comprising concentric circles into an output image of parallel lines. Mapping each input circle onto an output line gives the required deviation in ray direction and hence the phase profile of the transforming optical element. However, the resulting variation in optical path length means that the transformation introduces a phase distortion

that needs to be corrected by a second element. The transforming system therefore comprises two custom optical elements, one to transform the image and a second, positioned in the Fourier plane of the first, to correct for the phase distortion. This transformation is an example of an optical geometric transformation which has been previously studied in the context of optical image processing [19]. It was shown that a geometric transformation can only be implemented by a single optical element if the mapping is conformal. The optical element performs a mapping $(x, y) \mapsto (u, v)$, where (x, y) and (u, v) are the Cartesian coordinate systems in the input and output plane, respectively. In our approach $v = a \arctan(y/x)$ and the conformal mapping requires $u = -a \ln(\sqrt{x^2 + y^2}/b)$, similar to [20,21]. The phase profile of the transforming optical element is then given by

$$\phi_1(x, y) = \frac{2\pi a}{\lambda f}\left[y \arctan\left(\frac{y}{x}\right) - x \ln\left(\frac{\sqrt{x^2 + y^2}}{b}\right) + x \right], \quad (1)$$

where λ is the wavelength of the incoming beam, and f is the focal length of the Fourier-transforming lens. The parameter a scales the transformed image and $a = d/2\pi$, where d is the length of the transformed beam. b translates the transformed image in the u direction and can be chosen independently of a.

The required phase correction can be calculated by the stationary phase approximation [21] and is given by

$$\phi_2(u, v) = -\frac{2\pi ab}{\lambda f} \exp\left(-\frac{u}{a}\right)\cos\left(\frac{v}{a}\right), \quad (2)$$

where u and v are the Cartesian coordinates in the Fourier plane of the first element. Figures 1(a) and 1(b) show the phase profiles of the transforming and phase-correcting optical element, respectively. One can see that the transforming optical element contains a line discontinuity. The end of this line, i.e., the center of the phase profile, defines the axis around which the OAM is measured.

A lens is inserted after the phase-correcting element to focus the transformed beam, which now has a $2\pi\ell$ phase gradient, to a spot in its focal plane. In the plane of this lens, the transformed beam is rectangular, meaning that the diffraction limited focal spot is elongated in the direction orthogonal to the direction in which the spot moves. The transverse position of the spot changes as a function of ℓ and is given by

$$t_\ell = \frac{\lambda f}{d}\ell. \quad (3)$$

We use diffractive spatial light modulators (SLMs) to create the desired phase profiles. For monochromatic light, an SLM can be programmed such that any desired phase profile is applied to the first-order diffracted beam, limited in complexity only by the spatial resolution of the SLM. Figure 1(c) shows a schematic overview of the optical system. We use Laguerre-Gaussian (LG) beams as our
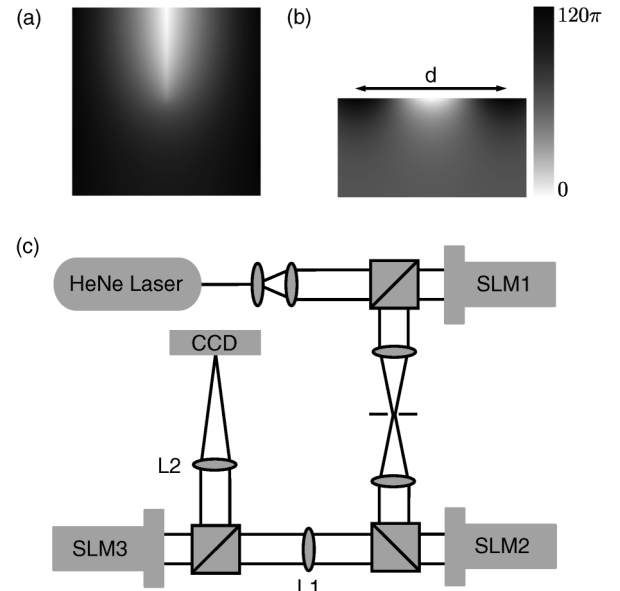

FIG. 1. Phase profiles of (a) the transforming and (b) the phase-correcting optical element. d is the length of the transformed beam. In (b) only that part of the phase-correcting element is shown, that is illuminated by the transformed beam. In the experiment, the phase profiles are displayed on the spatial light modulators (SLMs) with 2π phase modulation. (c) Schematic overview of the setup. We use SLMs to both generate Laguerre-Gaussian beams (SLM1) and create the desired phase profiles for the transforming and phase-correcting optical elements (SLM2 and SLM3, respectively). L1 is the Fourier-transforming lens and L2 focuses the transformed beams. We use beam splitters to ensure perpendicular incidence on the SLMs.

OAM states. The first SLM, programmed with both phase and intensity information [9], is used to generate any superposition of LG modes. Using relay optics and an iris to select the first-order diffracted beam, this input state is directed onto the transforming element, displayed on the second SLM, which performs the required geometrical transformation in the back focal plane of the Fourier-transforming lens. We choose d such that the transformed beam fills 80% of the width of the phase-corrector element in order to avoid diffraction effects at its edges. A third SLM is used to project the phase-correcting element. The diffracted beam from this SLM has a transverse phase gradient dependent on the input OAM state. These direction states are focused onto a CCD array by a lens and, as discussed above, the lateral position, t_ℓ, of the resulting elongated spots is proportional to the OAM state of the incident beam.

Figure 2 shows modeled and observed phase and intensity profiles at various places in the optical system for a range of OAM states. The modeled data are calculated by plane wave decomposition. In the second column, one can see that an input beam with circular intensity profile is unfolded to a rectangular intensity profile with a $2\pi\ell$ phase

gradient. As predicted, the position of the elongated spot changes with the OAM input state. We recorded the output of the mode sorter for input states between $\ell = -5$ and $\ell = 5$. The experimentally observed spot positions are in good agreement with the model prediction. Our system further allows us to identify a superposition of OAM states, as can be seen in the final row of Fig. 2, where an equal superposition of $\ell = -1$ and $\ell = 2$ gives two separate spots in the detector plane at the position of $\ell = -1$ and $\ell = 2$. We note that observed spots are slightly broader than the modeled ones, which is due to aberrations introduced by the optical system.

To directly measure the state of any input beam, we define eleven, equally sized, rectangular regions in the detector plane, all centered around one of the expected spot position for the eleven input modes used in the experiment. By measuring the total intensity in each of these
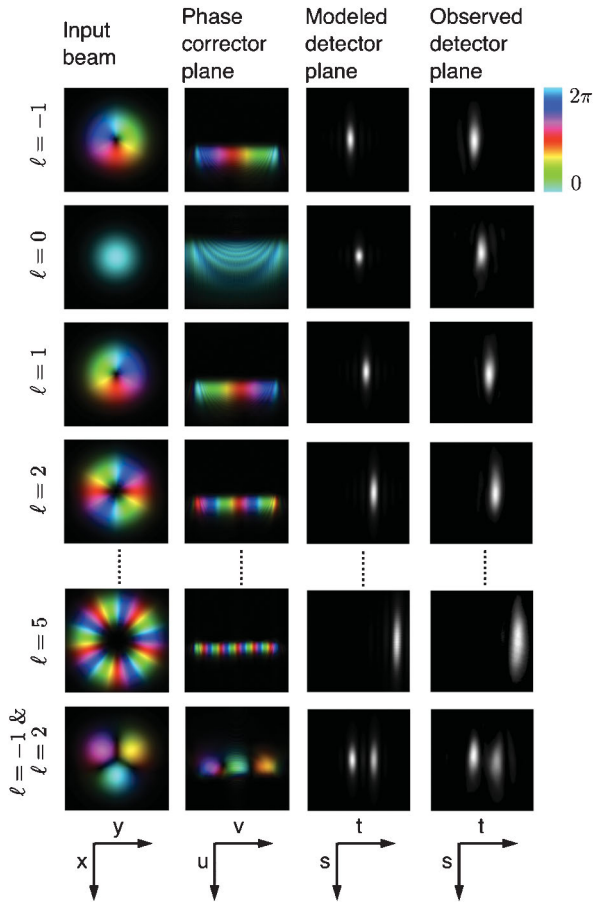

FIG. 2 (color). Modeled and observed phase and intensity profiles at various planes in the optical system. From left to right, the images show the modeled phase and intensity distribution of the input beam just before the transforming optical element and just after the phase-correcting element, and the modeled and observed images in the CCD plane for five different values of ℓ. The final row shows the results for an equal superposition of $\ell = -1$ and $\ell = 2$. The last two columns are $6\times$ magnified with respect to the first two columns.

regions, we can determine the relative fraction of a specific OAM state in the input beam. Figures 3(a) and 3(b) show the results for eleven pure input states, both modeled and observed, as shown in the third and fourth column of Fig. 2, respectively. Since the spots for two neighboring states slightly overlap, some of the light in a state leaks into neighboring regions; i.e., there is some cross talk between different states. This cross talk shows up as the off-diagonal elements in Fig. 3. As described before, our experimental results show slightly broader spots than the modeled data and hence the off-diagonal elements are slightly larger. It is clearly possible to determine the input state of the light beam from the position of the output spot in the detector plane.

A commonly used measure to quantify the amount of cross talk between channels is the channel capacity, which is the maximum amount of information that can be reliably transmitted by an information carrier [22]. In an optical system, this channel capacity can be quoted as "bits per photon." If a photon can be in one of N input states and its state can be measured perfectly at the output, the channel capacity takes the theoretical maximum value of $\log_2 N$.

Table I presents the channel capacity of the system for the modeled and observed results, calculated from the data shown in Fig. 3. A generic approach to minimize cross talk is to increase the separation between channels. We therefore consider the cases where we use only every other state, $\Delta \ell = 2$, and every third state, $\Delta \ell = 3$. This approach gives fewer states, but less overlap between different spots. In all cases, due to the experimental imperfections, the channel capacity for the observed data is slightly lower than the modeled one, but for $\Delta l = 3$ it approaches the model very closely.

We note that the optical transformation is only perfect for rays which are normally incident on the transforming element. Helically phased beams are inherently not of this type, the skew angle of the rays being ℓ / kr [23]. Although this skew angle is small when compared to the angles introduced by the transforming element, it might introduce a slight transformation error which increases with ℓ. If the input is a ringlike intensity profile, the skew angle leads to a sinusoidal distortion from the expected rectangular output. This potential skew ray distortion is reduced by

TABLE I. Channel capacity calculated from the results shown in Fig. 3. The first three columns show the separation between the channels, Δl, the number of states taken into account, N, and the theoretical maximum value, $\log_2 N$. The last two columns correspond to the data shown in Figs. 3(a) and 3(b), respectively.

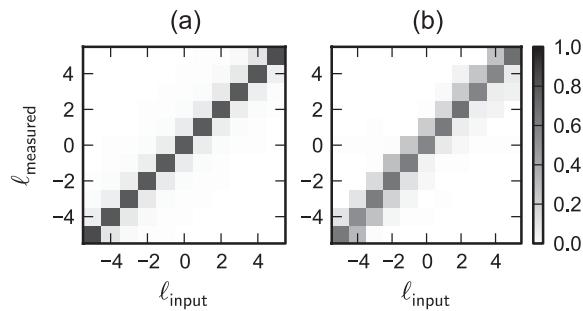| $\Delta \ell$	N	$\log_2 N$	Modeled	Observed
1	11	3.46	2.36	1.96
2	6	2.59	2.10	1.93
3	4	2.00	1.70	1.68

FIG. 3. Total intensities in all detector regions for pure input OAM states from $\ell = -5$ to $\ell = 5$, for both the (a) modeled and (b) observed results. The regions all have the same size and are chosen such that they fill the entire aperture. The intensities are shown as a fraction of the total intensity in the input beam.

decreasing the propagation distance over which the transformation occurs, i.e., reducing f.

In its present form, our approach is limited by the fact that the resulting spots are slightly overlapping. This is because our transformation discards the periodic nature of the angular variable, using instead only a single angular cycle and producing an inclined plane wave of finite width, and similarly a finite width of spot. One option for improvement is to modify the transformation to give multiple transverse cycles, which results in larger phase gradient and thus a larger separation between the spots, albeit at the expense of increased optical complexity. One approach to implementing this improvement would be to add a binary phase grating to the transforming elements, producing both positive and negative diffraction orders. By adjusting the pitch of the grating appropriately, two identical, adjoining copies of the reformatted image are created in the plane of the phase corrector.

We further recognize that there is a 70% light loss associated with the two SLMs that comprise the mode sorter. This loss could, however, be eliminated by replacing the SLMs with the equivalent custom-made refractive optical elements.

In conclusion, we have described a novel system comprising of two bespoke optical elements that can be used to efficiently measure the OAM state of light. We have shown numerical and observed data to support our method. The method has a limitation due to the overlap of the spots for different states that could be reduced by applying an additional diffraction grating to the first surface. The system opens the way to many interesting investigations ranging from experiments in multiport quantum entanglement [7],

to applications in astrophysics [24] and microscopy [25], all of which make use of the OAM state basis.

*j.berkhout@cosine.nl
†m.lavery@physics.gla.ac.uk

[1] L. Allen *et al.*, Phys. Rev. A **45**, 8185 (1992).
[2] G. Molina-Terriza, J. P. Torres, and L. Torner, Nature Phys. **3**, 305 (2007).
[3] S. Franke-Arnold, L. Allen, and M. Padgett, Laser Photon. Rev. **2**, 299 (2008).
[4] G. Molina-Terriza, J. P. Torres, and L. Torner, Phys. Rev. Lett. **88**, 013601 (2001).
[5] G. Gibson *et al.*, Opt. Express **12**, 5448 (2004).
[6] N. Bloembergen, J. Opt. Soc. Am. **70**, 1429 (1980).
[7] A. Vaziri, G. Weihs, and A. Zeilinger, Phys. Rev. Lett. **89**, 240401 (2002).
[8] J. T. Barreiro, T.-C. Wei, and P. G. Kwiat, Nature Phys. **4**, 282 (2008).
[9] J. Leach *et al.*, Science **329**, 662 (2010).
[10] V. Yu. Bazhenov, M. S. Soskin, and M. V. Vasnetsov, J. Mod. Opt. **39**, 985 (1992).
[11] N. R. Heckenberg *et al.*, Opt. Quantum Electron. **24**, S951 (1992).
[12] A. Mair *et al.*, Nature (London) **412**, 313 (2001).
[13] S. N. Khonina *et al.*, Opt. Commun. **175**, 301 (2000).
[14] M. Padgett *et al.*, Am. J. Phys. **64**, 77 (1996).
[15] G. C. G. Berkhout and M. W. Beijersbergen, Phys. Rev. Lett. **101**, 100801 (2008).
[16] J. M. Hickmann *et al.*, Phys. Rev. Lett. **105**, 053904 (2010).
[17] J. Courtial *et al.*, Phys. Rev. Lett. **81**, 4828 (1998).
[18] J. Leach *et al.*, Phys. Rev. Lett. **88**, 257901 (2002).
[19] O. Bryngdahl, J. Opt. Soc. Am. **64**, 1092 (1974).
[20] Y. Saito, S. Komatsu, and H. Ohzu, Opt. Commun. **47**, 8 (1983).
[21] W. J. Hossack and A. M. Darling, and A. Dahdouh, J. Mod. Opt. **34**, 1235 (1987).
[22] C. E. Shannon, Bell Syst. Tech. J. **27**, 379 (1948).
[23] M. J. Padgett and L. Allen, Opt. Commun. **121**, 36 (1995).
[24] M. Harwit, Astrophys. J. **597**, 1266 (2003).
[25] S. Fürhapter *et al.*, Opt. Express **13**, 689 (2005).